Full Wave Analysis of Propagation Characteristics of a Through Hole Using the Finite-Difference Time-Domain Method

Shuji Maeda, Tatsuya Kashiwa, *Member, IEEE*, and Ichiro Fukai, *Member, IEEE*

Abstract—**A full wave analysis of the propagation characteristics of a through hole (or via hole) was carried out using the finite-difference time-domain (FD-TD) method and results were compared with measurements from a physical model. The effects of rod diameter and microstrip connecting angle were examined. The computed scattering parameters (*S*-parameters) of a through hole showed excellent agreement with measured results from dc to high frequencies and in the time domain responses. As a result, it was shown that at high frequencies radiation is at a significant level and rod diameter and microstrip connecting angle strongly influence the propagation characteristics of a through hole.**

Introduction

THE MINIATURIZATION and ever higher density packing of electronic devices is driving a trend toward three-dimensional, multilayer circuits. At the same time, the clock rates in digital devices and the operating frequencies in communication systems are steadily increasing. In multilayer circuits, signals are carried between the layers by through holes [1]. The propagation characteristics of through holes have an ever stronger effect on the performance of electronic circuits as frequency increases. The through hole has a complex three dimensional structure consisting of microstrips, a rod, lands, and a clearance hole. Experiments with such structures become more difficult, time-consuming and expensive at high frequencies; however, it is necessary to predict the broad band characteristics of a through hole to estimate its performance.

Consequently, it is desirable to develop an accurate and efficient numerical model for through holes, but their complex structure has hampered quantitative analysis of their broad band propagation characteristics. The traditional numerical approaches [2] have lacked versatility and accuracy. Furthermore, investigations have not yet reported on the dependence of radiation losses upon the angle at which the microstrips on either side of the through hole meet (hereafter referred to as the microstrip connecting angle).

A time domain analysis method has the advantage that the broad band characteristics can be obtained in a single computer run using Fourier transforms. There are two main versatile and rigorous time domain simulation methods, the TLM (transmission line matrix) algorithm [3]–[4] and FD-TD (finite-difference time-domain) algorithm [5]–[8]. Both consist of full wave analyses. The FD-TD method is more suitable than the TLM method for this analysis because of its simplicity and efficiency.

This paper reports the propagation characteristics of a through hole using the FD-TD method. Especially, the effects of rod diameter and microstrip connecting angle are examined. There is a wide range of sizes of through holes in multilayer circuits, so the sizes of the through hole in this paper were selected for ease and accuracy of measurements and not in the intention of specifying some optimum. Still, the results obtained in this paper are probably of sufficient general nature to apply to all through holes. Results calculated according to the numerical model are compared with measurements from the physical model. As a result, it is shown that radiation is a significant factor at high frequencies. The frequency characteristics of the radiation depend on the microstrip connecting angle, rod diameter, and land diameter.

Numerical Approach

The FD-TD method has been successfully used for analysis in many kinds of electromagnetic problems [5]–[8]. In this method, the two Maxwell's curl equations are discretized both in time and space, and the field values on the nodal points of the lattice are calculated in a leap-frog algorithm.

In this analysis, a variable size mesh is used to reduce demands on memory and calculation time. It has already been confirmed that the connection error between variable meshes is negligible in the microstrip model.

Fig. 1 shows a diagram of the through hole model used in this analysis. It has three conductor layers. Microstrip A meets microstrip C at the angle θ, called the microstrip connecting angle. Rod B meets microstrip A and microstrip C at both lands. The clearance hole is large

Manuscript received April 1, 1991; revised July 26, 1991. This work was supported by Matsushita Electric Works, Ltd., Osaka, Japan.

S. Maeda is with the Material R&D Laboratory, Matsushita Electric Works, Ltd., 1048, Kadoma, Kadoma-shi, Osaka 571 Japan.

T. Kashiwa and I. Fukai are with the Faculty of Engineering, Hokkaido University, Sapporo 060 Japan.

IEEE Log Number 9103292.

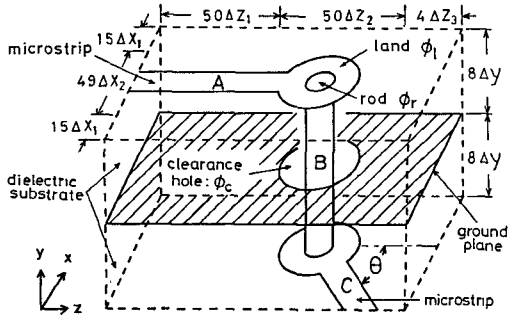

Fig. 1. Through hole in three multilayers. ($\epsilon_r = 3.4$, $\Delta x_1 = 0.3$ mm, $\Delta x_2 = 0.1$ mm, $\Delta y = 0.2$ mm, $\Delta z_1 = 0.3$ mm, $\Delta z_2 = 0.1$ mm, $\Delta z_3 = 0.3$ mm).

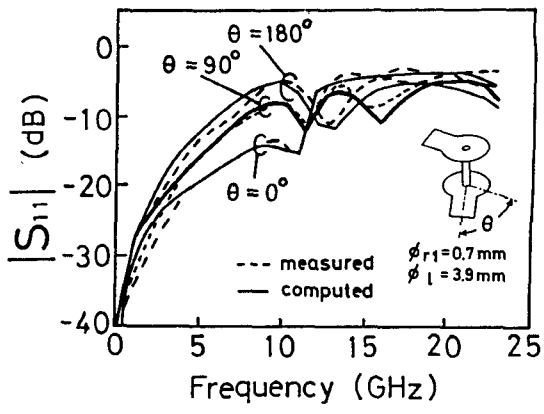

Fig. 2. $|S_{11}|$ versus frequency for three cases in which microstrip connecting angle is 0°, 90° and 180°. (Diameter of lands $\phi_1 = 3.9$ mm; diameter of rod $\phi_{r1} = 0.7$ mm).

enough to keep rod B out of contact with the ground plane and lined with a dielectric material. The inner region of rod B is filled with air. The center of the rod, lands, and clearance hold is at the point (x_1, z_1) of coordinates $x_1 = 15\Delta x_1 + 24.5\Delta x_2$ and $z_1 = 50\Delta z_1 + 25.5\Delta z_2$. There are assumed to be $16\Delta y$ height air regions over microstrip A and under microstrip C, but they are not shown in Fig. 1 for simplicity. To obtain accurate results, the spatial increments are chosen to be a fraction of the smallest wavelength. In this analysis, the spatial increments are chosen as $\Delta x_1 = 0.3$ mm, $\Delta x_2 = 0.1$ mm, $\Delta y = 0.2$ mm, $\Delta z_1 = 0.3$ mm, $\Delta z_2 = 0.1$ mm, and $\Delta z_3 = 0.3$ mm. The time increment is chosen as $\Delta t = 0.222$ps so as to satisfy the stability condition [6]. The staircasing approximation is used for modeling of the lands, clearance hole and rod conductor. The diameter of the lands ϕ_1 is 3.9 mm, the diameter of the clearance hole ϕ_c is 3.9 mm, and the diameter of the two rods tested are $\phi_{r1} = 0.7$ mm and $\phi_{r2} = 1.5$ mm. Each width of microstrip A and microstrip C is 3.3 mm. The substrate mainly consists of polyphenylene oxide (PPO) resin, which we have developed for microwave printed circuit boards. The permittivity of the substrate is assumed to be $\epsilon_r = 3.4$ at all frequencies [9]. In this analysis, dielectric loss and conductor loss are neglected, and the thickness of the conductor is considered zero for simplicity. On the xy-plane at $z = 4\Delta z_1$, a raised cosine pulse is applied under microstrip A in Fig. 1. The calculated electric field component (E_y) follows this form (1):

$$E_y = 1 - \cos(2\pi f_{\text{band}} t): \qquad 0 < t < 1/f_{\text{band}}$$
$$E_y = 0: \qquad 1/f_{\text{band}} < t$$
$$f_{\text{band}} = 12.0\ (\text{GHz}). \tag{1}$$

The time histories of voltage waves were calculated by integrating the E_y component between the ground plane and microstrip at the specified points. The time history of the reflected wave at the point (x_{ar}, z_{ar}) where $x_{ar} = 15\Delta x_1 + 25\Delta x_2$ and $z_{ar} = 2\Delta z_1$ were recorded. The time history of the original incident wave was recorded for the point $x_{ai} = 15\Delta x_1 + 25\Delta x_2$ and $z_{ai} = 21\Delta z_1$. The time histories of transmitted waves were recorded at different locations, depending on the microstrip connecting angle θ. When $\theta = 0°$, the observation point corresponded to $x_{c1} = 15\Delta x_1 + 25\Delta x_2$, $z_{c1} = 50\Delta z_1 + 50\Delta z_2 + 2\Delta z_3$. For $\theta = 90°$, the observation point corresponded to $x_{c2} = 13\Delta x_1$, $z_{c2} = 50\Delta z_1 + 25\Delta z_2$. For $\theta = 180°$, the observation point corresponded to $x_{c3} = 15\Delta x_1 + 25\Delta x_2$, $z_{c3} = 2\Delta z_1$. The obtained data were fast Fourier transformed and normalized in terms of the incident wave spectrum to obtain S-parameters $S_{11}(\omega)$ and $S_{21}(\omega)$. Those were defined as

$$S_{11}(\omega) = V_{\text{ref}}(\omega)/V_{\text{inc}}(\omega)$$
$$S_{21}(\omega) = V_{\text{out}}(\omega)/V_{\text{inc}}(\omega), \tag{2}$$

where $V_{\text{ref}}(\omega)$ is the reflection voltage, $V_{\text{inc}}(\omega)$ is the incident voltage, and $V_{\text{out}}(\omega)$ is the transmission voltage. The first order absorbing boundary condition [10], [11] is adopted on the surfaces of the analyzed region. The authors have confirmed that reflections from absorbing boundaries may be neglected.

Results and Discussion

The authors first investigated the frequency dependency of S-parameters $|S_{11}|$ and $|S_{21}|$ of a through hole using the FD-TD method; afterward, the time response of a through hole was examined.

First, we described the effect of the microstrip connecting angle on S-parameters.

Figs. 2 and 3 show the magnitude of $|S_{11}|$ and $|S_{21}|$, respectively, for the cases in which the microstrip connecting angle is 0°, 90°, and 180°. In order to verify the computed results, we measured the S-parameters using a network analyzer. The rod diameter of the through hole in the experiment was $\phi_{r1} = 0.74$ mm. The diameter of the land and clearance hole was about 3.9 mm. The computed results showed good agreement with the measured ones from dc to high frequencies. For $\theta = 180°$, the measured result is a little different from the computed one; this may be because coupling between connectors located at the same front of the through hole occurs at high frequencies. In this figure, $|S_{21}|$ generally drops with increase in frequency for $\theta = 0°$ and $\theta = 180°$. It seems that low frequency waves propagate well, but high fre-

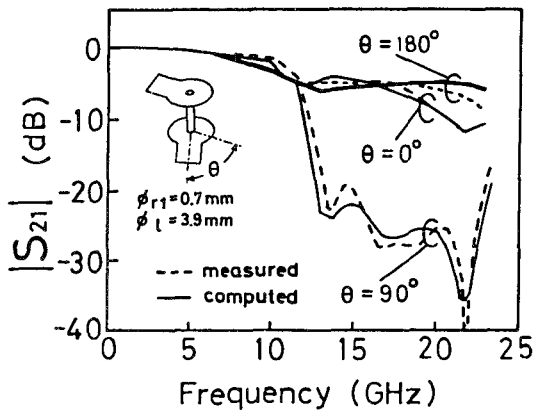

Fig. 3. $|S_{21}|$ versus frequency for three cases in which microstrip connecting angle is 0°, 90°, and 180°. (Diameter of lands $\phi_1 = 3.9$ mm; diameter of rod $\phi_{r1} = 0.7$ mm).

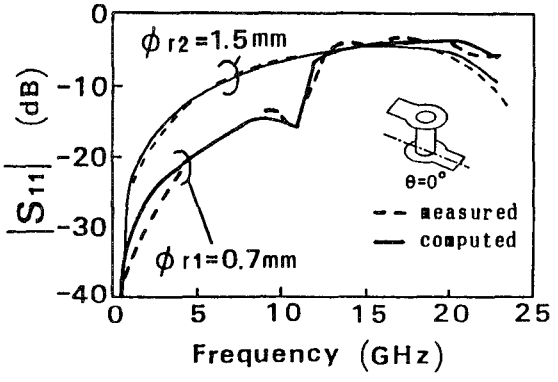

Fig. 4. $|S_{11}|$ versus frequency; the effect of rod diameter. (Microstrip connecting angle $\theta = 0°$; diameter of rods $\phi_{r1} = 0.7$ mm, $\phi_{r2} = 1.5$ mm; diameter of lands $\phi_1 = 3.9$ mm).

quency waves do not. For $\theta = 90°$, $|S_{21}|$ drops suddenly at about 12 GHz. Waves over 12 GHz probably do not propagate well because $|S_{21}|$ continues to be under -20 dB.

In this paper, the effect of the rod diameter was examined only for the case of $\theta = 0°$. The diameter of the rod used in the experiment was $\phi_{r1} = 0.74$ mm and $\phi_{r2} = 1.58$ mm.

Fig. 4 shows the magnitude of the reflection coefficient $|S_{11}|$ for microstrip connecting angle $\theta = 0°$. Fig. 5 shows the magnitude of transmission coefficient $|S_{21}|$ for $\theta = 0°$. The computed results show excellent agreement with the measured ones from dc to high frequencies. It is clear that the frequency characteristics of S-parameters depend on the diameter of a through hole.

A complex structure such as a through hole tends to emit a significant amount of radiation. From Figs. 2 and 3, it is clear that the energy conservation is not satisfied between input and output power. We examined the radiation power.

Figs. 6–8 show the computed radiation power P_c in the simulation, and the measured value $P_m = 1 - |S_{11}|^2 - |S_{21}|^2$ from the experimental data $|S_{11}|$ and $|S_{21}|$ for the through hole structures mentioned above. The radiation P_c was

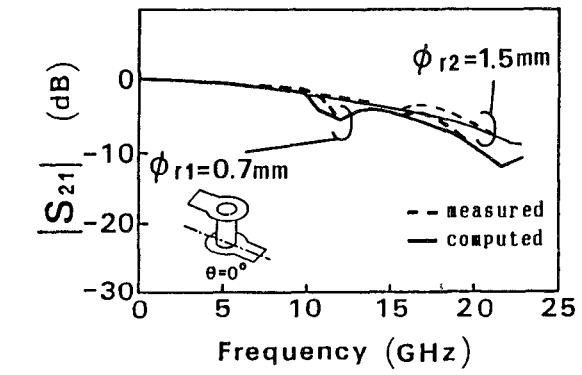

Fig. 5. $|S_{21}|$ versus frequency; the effect of rod diameter. (Microstrip connecting angle $\theta = 0°$, diameter of rods $\phi_{r1} = 0.7$ mm, $\phi_{r2} = 1.5$ mm, diameter of lands $\phi_1 = 3.9$ mm).

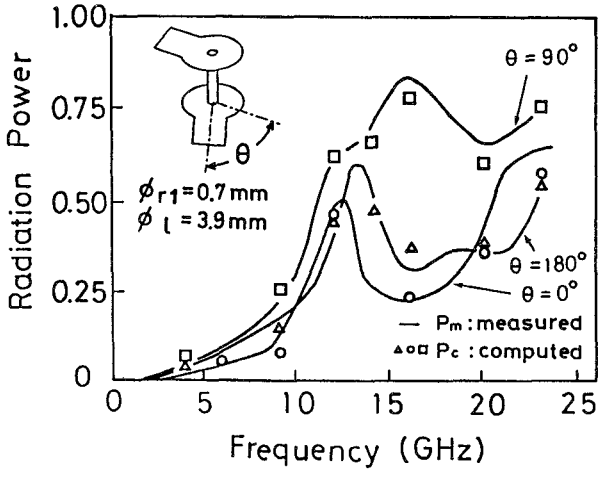

Fig. 6. Radiation power versus frequency for three cases in which microstrip connecting angle is 0°, 90°, and 180°. (Diameter of lands $\phi_1 = 3.9$ mm; diameter of rod $\phi_{r1} = 0.7$ mm).

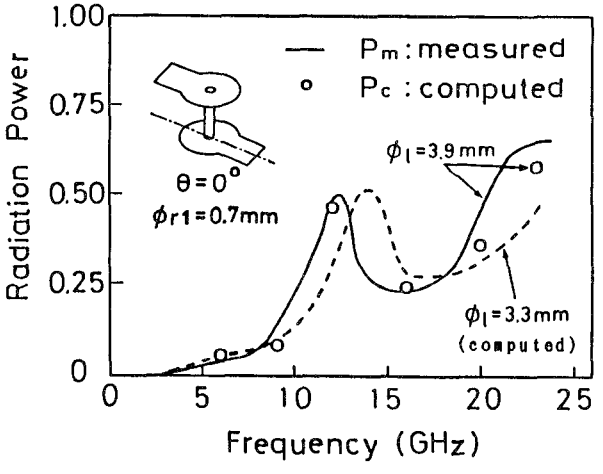

Fig. 7. Radiation power versus frequency; the effect of land diameter. (Microstrip connecting angle $\theta = 0°$; diameter of lands $\phi_1 = 3.9$ mm, $\phi_1 = 3.3$ mm; diameter of rod $\phi_{r1} = 0.7$ mm).

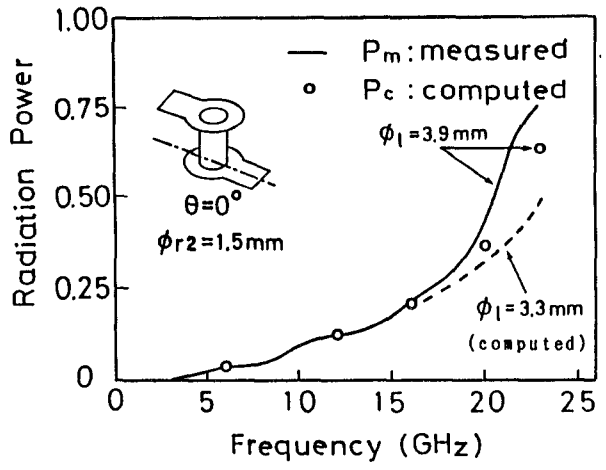

Fig. 8. Radiation power versus frequency; the effect of land diameter. (Microstrip connecting angle $\theta = 0°$; diameter of lands $\phi_1 = 3.9$ mm, $\phi_1 = 3.3$ mm; diameter of rod $\phi_{r2} = 1.5$ mm).

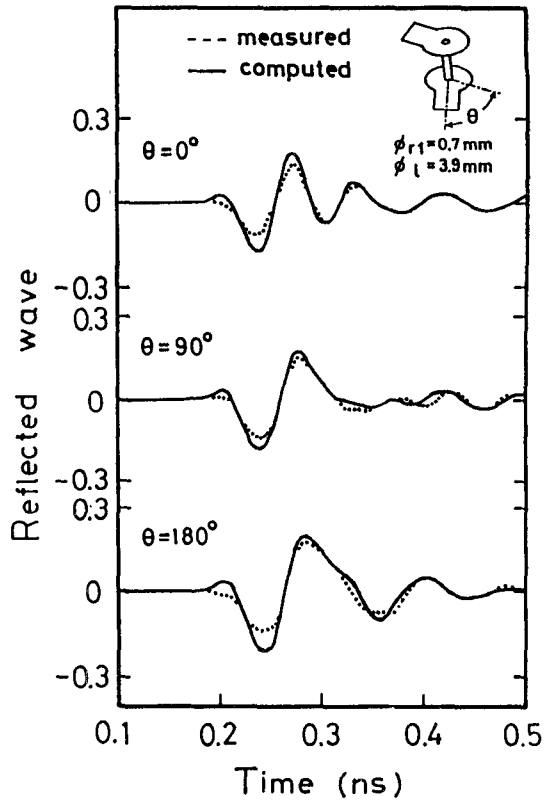

Fig. 9. Time response of reflected wave for three cases in which microstrip connecting angle is 0°, 90°, and 180°. (Diameter of rod $\phi_{r1} = 0.7$ mm; diameter of land $\phi_1 = 3.9$ mm).

calculated using the Poynting's vector in the rectangular parallelepiped surfaces surrounding the through hole. In this simulation, we confirmed that the energy conservation law is satisfied in terms of $|S_{11}|, |S_{21}|$ and radiation power P_c. Agreements with P_c in Figs. 6–8 indicate that the lost energy P_m in the measurement corresponds to the radiation power.

Fig. 6 shows the effect of the microstrip connecting angles. In Fig. 6, the rod diameter is $\phi_{r1} = 0.7$ mm, the land diameter is $\phi_1 = 3.9$ mm, and the microstrip line connecting angles are 0°, 90°, and 180°. The radiation strongly depends on the structure of the microstrip connecting angle at the through hole. The through hole with $\theta = 90°$ radiated more strongly than the holes with other microstrip connecting angles. The input microstrip line has a symmetrical structure, but the through hole part has an asymmetrical one. Consequently, stronger electromagnetic waves were radiated to fit the boundary condition. For $\theta = 0°$ and $\theta = 180°$, the peaks appeared at about 12.5 GHz. For $\theta = 90°$, a small peak occurred at about the same frequency. The reason is considered the resonance of the land of this diameter, as will be described below.

Fig. 7 shows the effect of land diameters for two cases in which the land diameter is $\phi_1 = 3.9$ mm and $\phi_1 = 3.3$ mm. In Fig. 7, the rod diameter $\phi_{r1} = 0.7$ mm and the microstrip connecting angle is $\theta = 0°$. The radiation frequency shows two peaks corresponding to each land diameter. When the land diameter was 3.9 mm, a radiation peak appeared at about 12.2 GHz (the solid line in the figure). When the diameter of the land was 3.3 mm, the peak computed at about 14.0 GHz (the dotted line in the figure). The ratio of peak frequencies is almost equal to the inverse ratio of the land diameters. This implies that the radiation is mainly caused by resonance of the lands. This phenomenon corresponds to the dip at the same frequencies in Figs. 2 and 3.

Fig. 8 shows the effect of land diameters for two cases in which the land diameter is $\phi_1 = 3.9$ mm and $\phi_1 = 3.3$ mm. In Fig. 8, the rod diameter $\phi_{r2} = 1.5$ mm and the connecting angle is $\theta = 0°$. No radiation peak appeared for different diameters of lands with this larger rod.

Second, we computed the time response.

Figs. 9 and 10 show the dependency of microstrip connecting angles in time domain pulse responses for the reflected and the transmitted waves. There was a small difference in magnitude between the measured and computed values; the reason for this was the attenuation at the connections from the coaxial lines to the microstrips at each end of the DUT (device under test). For $\theta = 180°$, it was difficult to reduce the coupling between connectors located at the same front of the DUT precisely in the physical model. In contrast, the simulation provided accurate results for ideal states. In Figs. 9 and 10, the width of the reflected and transmitted waves increased with the increment of microstrip connecting angle. The wave forms varied significantly according to the connecting angles.

Figs. 11 and 12 show the dependency of rod diameter in the time domain pulse responses of the through hole with a $\theta = 0°$ microstrip connecting angle. In Figs. 11 and 12, the rod diameters are $\phi_{r1} = 0.7$ mm and $\phi_{r2} = 1.5$ mm. The computed results for the wave form showed good agreement with the measured ones. The small differences in the magnitude which appeared between the measured and computed values were due to the attenuation described above. The reflected wave form changed from minus to plus. This wave form shows that this through hole structure has the characteristics of the shunt C type.

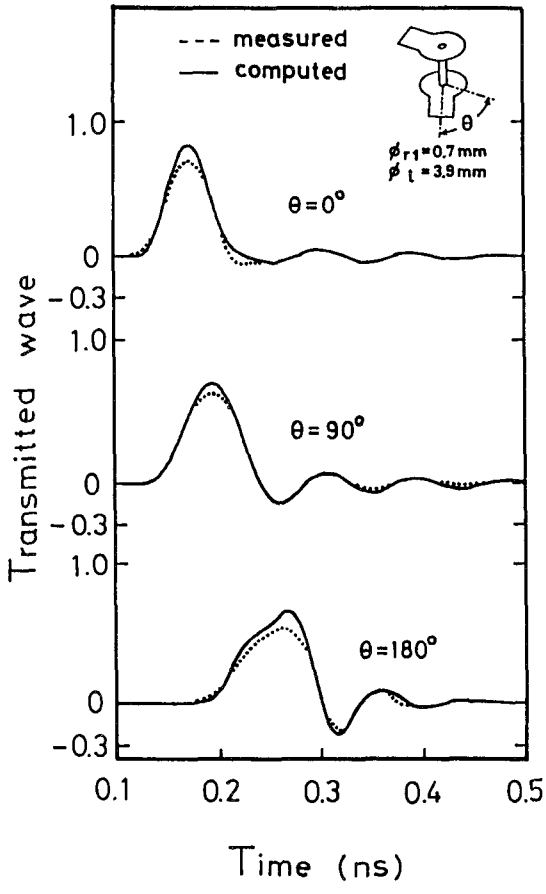

Fig. 10. Time response of transmitted wave for three cases in which microstrip connecting angle is 0°, 90°, and 180°. (Diameter of rod $\phi_{r1} = 0.7$ mm; diameter of land $\phi_1 = 3.9$ mm).

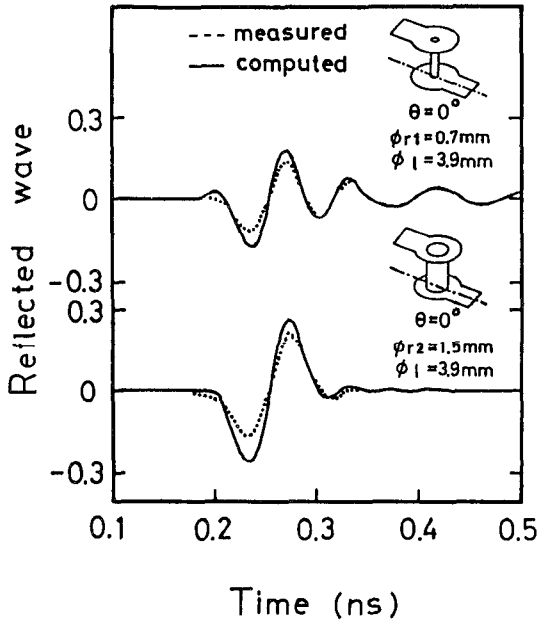

Fig. 11. Time response of reflected wave; the effect of rod diameter. (Microstrip connecting angle $\theta = 0°$; diameter of rods $\phi_{r1} = 0.7$ mm, $\phi_{r2} = 1.5$ mm; diameter of lands $\phi_1 = 3.9$ mm).

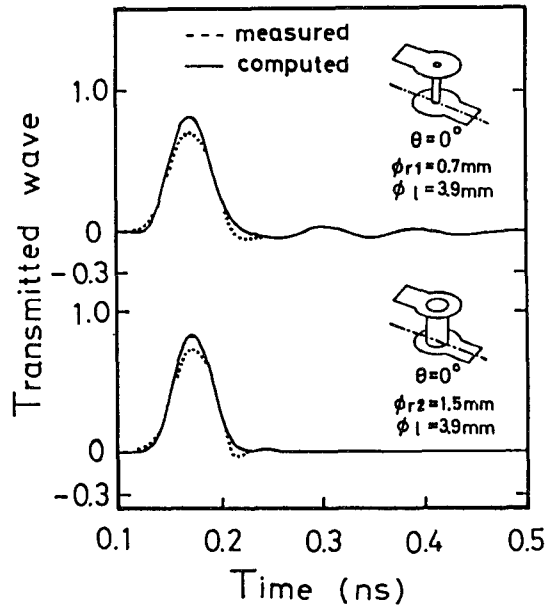

Fig. 12. Time response of transmitted wave; the effect of rod diameter. (Microstrip connecting angle $\theta = 0°$; diameter of rods $\phi_{r1} = 0.7$ mm, $\phi_{r2} = 1.5$ mm, diameter of lands $\phi_1 = 3.9$ mm).

The computations were executed on a Hitachi S820/80 supercomputer. The CPU time for the simulation was about 140 seconds. The memory size was about 20 Mbytes.

Conclusion

A full wave analysis of the propagation characteristics of a through hole of a complex three dimensional structure was carried out using the FD-TD method, and these results were compared with data from physical models. The computed results showed excellent agreement with the measured results from dc to the high frequency region and for various microstrip connecting angles. Radiation at a through hole is clearly not a negligible factor for high frequencies. The radiation effect strongly depends upon the microstrip connecting angle. At microstrip connecting angle $\theta = 90°$, the radiation of the through hole was stronger than for $\theta = 0°$ and 180°. From the time response of reflected waves in this analysis, the shunt C factor seems to increase with the decrease of the rod diameter within the region of the parameters in this investigation. It is considered that the results obtained in this paper are sufficiently general to apply to most through holes. The results show the validity and effectiveness of the simulation using the FD-TD method for analyzing the through hole. Thus, this approach can be useful for optimizing some through hole structures.

Simulation can efficiently provide quantitative and accurate physical values which are difficult to measure directly, such as radiation phenomena. Furthermore, simulations considerably eases evaluation of ideal electromagnetic properties in comparison with experiments, into which can creep disturbing factors such as faulty coupling between elements, environmental influences, etc. The recent development in computers has enabled the efficient

design of complex microwave structures through simulations replacing traditional complicated experiments.

ACKNOWLEDGMENT

The authors wish to thank T. Sakamoto and M. Kawai of the Matsushita Electric Works, Ltd. for encouraging this work.

REFERENCES

[1] C. F. Coombs, Jr., *Printed Circuits Handbook*, 3rd ed. New York: McGraw-Hill, ch. 31, 1988.
[2] E. Takagi, T. Onojima, and M. Konno, "The characteristics of a via hole in high frequency region," in *Nat. Conf. IEICE Japan Rec.*, vol. 5, 1989, p. 226.
[3] N. Masuzuka, N. Yoahida, and I. Fukai, "Transient analysis of three-dimensional electromagnetic field in through-hole," *Trans. IEICE Japan*, vol. E70, no. 8, pp. 703–705, Aug. 1987.
[4] S. Akhtarzad and P. B. Jones, "Solution of Maxwell's equations in three space dimensions and time by the t.l.m. method of numerical analysis," *Proc. IEE*, vol. 122, no. 12, pp. 1344–1348, Dec. 1975.
[5] K. S. Yee, "Numerical solution of initial boundary value problems involving Maxwell's equations in isotropic media," *IEEE Trans. Antennas Propagat.*, vol. AP-14, pp. 302–307, May 1966.
[6] A. Taflove, "Review of the formulation and applications of the finite-difference time-domain method for numerical modeling of electromagnetic wave interactions with arbitrary structure," *Wave Motion*, vol. 10, pp. 547–582, Dec. 1988.
[7] X. Zhang, J. Fang, K. Mei, and Y. Liu, "Calculation of the dispersive characteristics of microstrips by the time-domain finite difference method," *IEEE Trans. Microwave Theory Tech.*, vol. MTT-36, no. 2, pp. 263–267, Feb. 1988.
[8] I. Wolff, "From approximation to a three-dimensional full-wave solution of planar line discontinuities for microwave integrated circuits," in *European Microwave Conf. Rec.*, vol. A5.1, pp. 123–140, Sep. 1990.
[9] T. Kashiwa, Y. Ohtomo, and I. Fukai, "A finite-difference time-domain formulation for transient propagation in dispersive media associated with cole-cole's circular arc law," *Microwave and Optical Tech. Lett.*, vol. 3, no. 12, pp. 416–419, Dec. 1990.
[10] G. Mur, "Absorbing boundary conditions for the finite-difference approximation of the time-domain electromagnetic-field equations," *IEEE Trans. Electromagn. Compat.*, vol. EMC-23, no. 4, pp. 377–382, Nov. 1981.
[11] D. M. Sheen, S. M. Ali, M. D. Abouzahra, and J. A. Kong, "Application of the three-dimensional finite-difference time-domain method to the analysis of planar microstrip circuits," *IEEE Trans. Microwave Theory Tech.*, vol. MTT-38, no. 7, pp. 849–857, July, 1990.

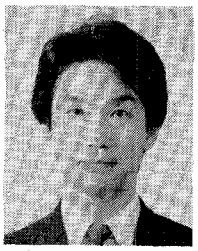

Shuji Maeda was born in Tottori, Japan, on March 21, 1958. He received the B.E. and M.E. degrees in materials science and engineering from the University of Electro-Communications, Chofu, Japan, in 1981 and 1983, respectively.

He joined the Matsushita Electric Works, Ltd., Osaka in 1983, where he worked in the Material Research and Development Laboratory for the development of materials for microwave printed circuit boards. From 1989 to 1991 he did research at Hokkaido University, Sapporo, Japan.

Mr. Maeda is a member of the Institute of Electronics, Information and Communication Engineers in Japan.

Tatsuya Kashiwa (M'88) was born in Hokkaido, Japan, on June 3, 1961. He received the B.E. and M.E. degrees in electrical engineering from Hokkaido University, Sapporo, Japan, in 1984 and 1986, respectively.

He became a Research Assistant in the same university in 1988. His research interests include analysis of anisotropic media and antennas.

Mr. Kashiwa is a member of the Institute of Electronics, Information and Communication Engineers in Japan.

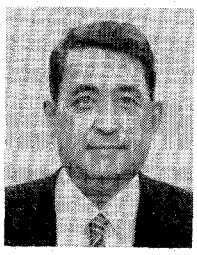

Ichiro Fukai (M'87) was born in Hokkaido, Japan, on August 21, 1930. He received the B.E., M.E., and D.E. degrees in electrical engineering from Hokkaido University, Sapporo, Japan in 1953, 1956, and 1976 respectively.

In 1956, he joined the Defense Agency Technical Research and Development Institute. He became a Research Assistant in 1959 in the Faculty of Engineering of Hokkaido University and an Associate Professor at the Technical Teacher's Training Institute in 1961. In 1968 he became an Associate Professor and in 1977 a Professor in the Department of Electrical Engineering at the same university.

Dr. Fukai is a member of the Institute of Electrical Engineers of Japan and of the Institute of Electronics, Information and Communication Engineers in Japan.